

Feasibility Study of a PLC System for Avionic Safety-Critical Systems

Thomas Larhzaoui, Fabienne Nouvel, Jean-Yves
Baudais

IETR

Rennes, France

thomas.larhzaoui@insa-rennes.fr, fabienne.nouvel@insa-
rennes.fr, jean-yves.baudais@insa-rennes.fr

Virginie Degardin, Pierre Laly

IEMN, TELICE

Lille, France

virginie.degardin@univ-lille1.fr, pierre.laly@univ-lille1.fr

Abstract— To increase the flexibility of the aircraft equipments and to reduce the possession and operating costs of the aircrafts, the main aircraft manufacturers want to change fluidic systems by electrical systems. However, this evolution induces a high increase of the number of wires. Reducing the amount of wiring also allows decreasing the construction and the maintenance costs, and the polluting emissions. Another interest is improving the reliability of aircraft equipment such as allowing monitoring of power cables. To limit the number wires, we proposed to use power line communication (PLC) for flight control systems (FCS) on the high voltage direct current network (HVDC), between a calculator unit and a power inverter for medium-haul aircrafts. PLC technology has proven its reliability for indoor network with the Homeplug Av standard. Nowadays, many studies deal with the possibility to use PLC for embedded systems. However, PLC for safety-critical avionic systems are not often studied. This paper attempts to define the physical layer for such application. The proposed transmission technique used is orthogonal frequency division multiplexing (OFDM), which is widely used with success in many telecommunication systems. In this paper, we present throughput measurement with Homeplug Av modems to prove the feasibility of PLC in aircraft environment. However, the Homeplug Av parameters are not adapted to the aeronautic constraints. Based on channel transfer function measurements and analysis, we proposed to adapt the OFDM parameters to comply with the FCS real-time constraints.

Keywords-PLC; OFDM; coherence bandwidth; delay spread; insertion gain; channel impulse response; aircraft; avionic; bit rate; safety critical systems; HVDC network.

I. INTRODUCTION

In future aircrafts, hydraulic flight control systems (FCS) will be replaced by electric ones. The main interests are a better flexibility and a decrease in maintenance costs. However, the major problem is the increasing of wires length. Since the actuators for the FCS are electrical actuators, it is possible to change the medium to improve the speed of the transmissions, the reliability or to decrease the complexity of the electrical network. To reduce the electrical network complexity and propose a reliable transmission in the medium-haul aircrafts, PLC technology seems to be a good candidate.

Reducing the mass of wiring also has the benefit of reducing not only the maintenance and the construction costs, but also the polluting emissions. In addition, the PLC technology could improve the reliability of the aircraft equipment through the monitoring of the power wires. In previous work [1], we proposed to define OFDM parameters for such kind of transmission in order to comply with the real-time constraints. It is also possible to use optical fibers for the FCS, which is called fly-by-light [2]. They allow high data rates and fast transmissions. However, it does not solve the problems of the network complexity, and aircraft manufacturers remain reluctant to use them for avionics critical systems due to the maintenance constraints. Another possibility is to use wireless communication which is called fly-by-wireless [3]. The main advantage of this technology is that it removes the wired medium. However, this technology is vulnerable from the electromagnetic point of view, in terms of safety and reliability.

PLC technology has proven its reliability in in-home network with HomePlug Av [4]. This standard allows to transmit data with a bit rate of about 200 Mbit/s in the [1;30] MHz bandwidth. In addition, there are numerous studies concerning PLC in different kinds of vehicles like cars [5][6][7][8], ships [10][11], and trains [12][13]. PLC technology is also investigated in aircraft cabin lighting system for multimedia application in the European project TAUPE [14][15]. However, even if the cabin lighting system network is representative of one part of the aircraft electrical network, it is not appropriate for safety-critical systems like FCS. A first study, which proposed to use PLC for a critical system, has been done in [16]. The authors studied the feasibility of using PLC technology between the power inverter and the actuator for landing gears. In this case, the wire length between the power inverter and the actuator is about five meters and the network is a non-filtered low voltage AC network. Nevertheless, in this paper, we focus on a new high voltage direct current (HVDC) network, which is longer (until thirty two meters long) and filtered. The HVDC network is a new ± 270 VDC power supply network, which will replace the AC 115 V, 400 Hz network.

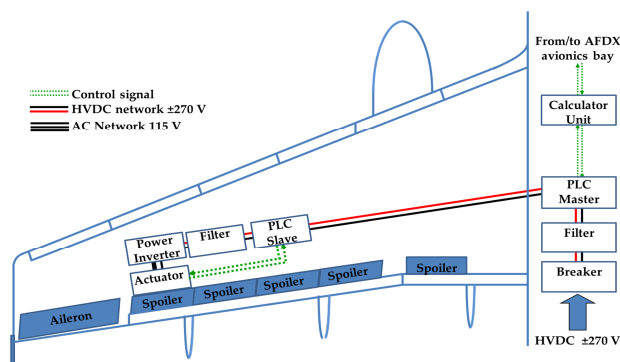


Figure 1. PLC system on aircraft wing

The interest for the aircraft manufacturers to use a HVDC network is to allow the simplification of the power networks (alternators, power conversion, circuit breakers, etc.). It becomes possible to use the reversibility of the electrical actuators for the FCS to produce electrical power. As the HVDC network is still in design, we can influence the design of the power network in order to improve the quality of the propagation channel for the proposed PLC transmissions.

FCS do not require a high bit rate link, few Mbit/s being enough. Nevertheless, the communication must be highly reliable, deterministic, real time and must comply with the DO-160 [17]. The DO-160 specifies test conditions for the design of avionics electronic hardware in airborne systems. As shown in Fig. 1, we consider the link between the calculator unit and the power inverter located near the actuators used for flight control. In this illustration, the PLC master near the calculator unit transmits data to the PLC slave near the power inverter. It corresponds to a point-to-point topology. It is also possible to use point-to-multipoint topology, where one PLC node transmits data to two PLC nodes. Moreover, one of the major challenges of the command of the FCS is the real time constraints. The FCS operates at frequency about 1 kHz, which is called the fast control loop. According to the common practice for the aeronautic equipment, command systems must work six times faster than the equipment that they command. It represents a 6 kHz frequency system or a 167 μ s period in this scheme. However, there are several calculators in this fast control loop, which require time processing. It seems reasonable to consider that the PLC system time processing of the must not exceed from 10 % to 20 % of the 167 μ s period. In our case, it varies from 17 μ s to 34 μ s.

The proposed PLC data transmissions are based on the OFDM technique [18], which has been used with success in many wireless and wired line communication systems like DVB, indoor PLC standards or 3GPP-LTE. This technology is interesting for the PLC transmission because it is flexible and robust in frequency selective channels.

In this paper, we measure and analyze the propagation channel in order to define an OFDM symbol duration in compliance with the real-time constraints. Bit rate measurements are also performed to prove the feasibility of the PLC on the HVDC network for the FCS.

This paper is organized as follows. In Section II, we describe the channel and the test bench, while results on the insertion gain are presented in Section III. Section IV describes the channel analysis and the optimization of the OFDM parameters is presented in Section V. In Section VI, simulations are performed in order to check the parameters proposed in the previous section. The bit rate measurements of the PLC link are given in Section VII. A synthesis of the main results and a conclusion are given in Section VIII.

II. DESCRIPTION OF THE TEST BENCH AND OF THE MEASUREMENT CONFIGURATION

In the test bench, the channel is composed of a harness and two couplers that allow to connect the communication system over the HVDC network. Two kinds of couplers are used: capacitive couplers or inductive couplers.

A. Harnesses Configuration

During the measurement campaign, three architectures were studied:

- the point-to-point architecture, with two capacitive couplers: architecture 1 (Fig. 2),
- the point-to-point architecture, with two inductive couplers: architecture 2 (Fig. 3),
- the point-to-multipoint architecture with one master and two slaves, architecture 3 (Fig. 4).

The tests have been performed on a test bench with active loads which are representative of actual avionic loads and with a ± 270 DC power supply. A fan has also been used. For this experiment, a harness of 32 meters long is used. It is representative of one possible wire length of the power network of the FCS in aircrafts. It includes one twisted pair, one twisted quadrifilar cable, and one single wire.

In Fig. 2, the architecture 1 is represented. Capacitive couplers are used to transmit on one twisted pair over +270 V and -270 V. Capacitive couplers are composed by a transformer for the galvanic isolation and two capacitors. The harness is composed by one twisted pair. We have also considered another possibility, i.e., to use a twisted quadrifilar for two different transmissions on the two polarities for the same load. In this case, the quadrifilar is short circuited at both ends of each polarity and inductive couplers can be used as illustrated in the architecture 2 in Fig. 3. In this figure, one signal is transmitted on the pair on the +270 V and one other signal is transmitted on the other pair on the -270 V. It must be emphasized that, for the same DC power, the diameter of each wire of the quadrifilar can be reduced to avoid an increase of the copper weight.

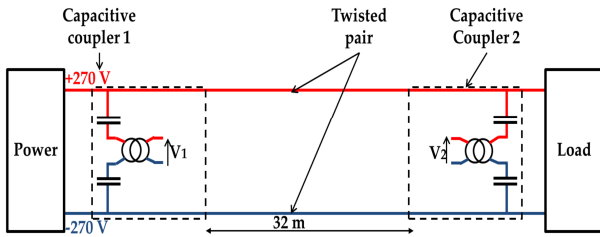


Figure 2. Point-to-point architecture with capacitive coupler

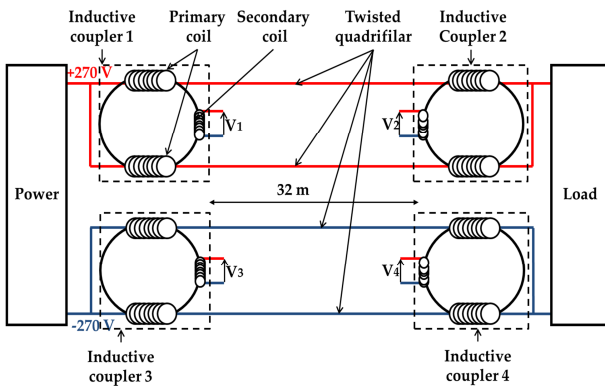


Figure 3. Point-to-point architecture with inductive coupler

There are two main interests to use this architecture. First, due to the short circuits at both ends, the communications are less disturbed by the noise produced by the power supply and the load. The other one is the possibility to use the avionics full duplex (AFDX) twisted quadrifilar already used in aircrafts for the transmissions [19]. These quadrifilars are light and their conception is mature. It means that the physical characteristics of the wires and the connectors are well known, which is the major asset for the implantation in the aircrafts. In addition, this architecture allows different possibilities of transmission. For example, it is possible to use the second polarity for redundancy or use the four couplers for a full duplex transmission.

The architecture 3 is presented in Fig. 4. In this case, three couplers are used on the +270 V. Thus, the harness is composed of one quadrifilar and one wire for the -270 V polarity. Such architecture allows to test the case where one effector as an aileron is driven by two actuators (loads). For the architecture 3, only the transmission on the +270 V polarity has been tested. It is necessary to test the point-to-multipoint topology because the transfer function cannot be deduced from the point-to-point architecture due to the multipath and crosstalk. But, similarly to the architecture 2, it is possible to consider a transmission on both polarities for two loads for the explorations of different possibilities of transmissions.

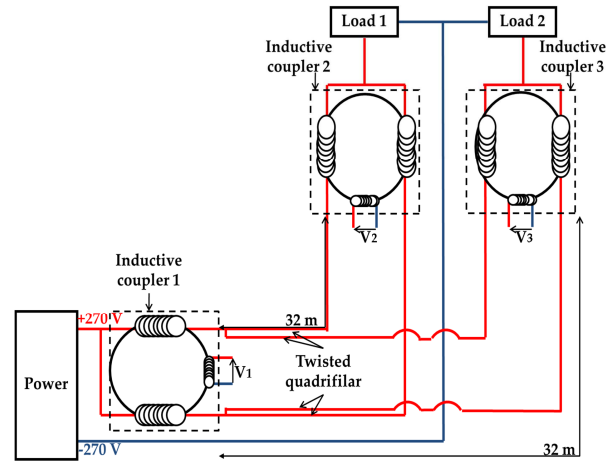


Figure 4. Point-to-multipoint architecture with inductive coupler

B. Channel Measurements

Transfer function measurements have been carried out with a network analyser in the [1;100] MHz bandwidth with a 5 kHz resolution bandwidth. To do this, we used the frequency scanning method. This technique involves scanning the channel using a network analyser with a constant step Δf on a frequency bandwidth equal to $f_0 + N\Delta f$, where f_0 is the minimum frequency, Δf is the frequency step, and N is the number of measurement points. For each configuration, the transfer functions have been measured between the input and the output V_1 , V_2 , V_3 and V_4 . Since there are more than two couplers on the architectures 2 and 3, 50 Ω loads are connected on the non used couplers during the transfer function measurements.

III. PRELIMINARY RESULTS

In order to prove the PLC feasibility and measure the throughput on the test bench, Homeplug Av modems have been plugged on the architectures 1 and 2 through the couplers. The power supply of the modems comes from the HVDC network via a DC/DC converter. Data transmissions between couplers and modems are done by a twisted pair. In this preliminary study, we just focus on the experimental aspects to obtain a first result on link capabilities using product on the shelf.

The throughput measurements are shown in Fig. 5 and have been performed with the Jperf software. When the network is turned off, the throughput achieved 40 Mbit/s for both architectures. The tests with the active loads show a small decrease of the throughput. The tests with the fan, which is noisy, show the interest of the inductive coupler compared with the capacitive coupler. Indeed, the throughput does not change a lot with the inductive coupler but is divided by two with the capacitive coupler.

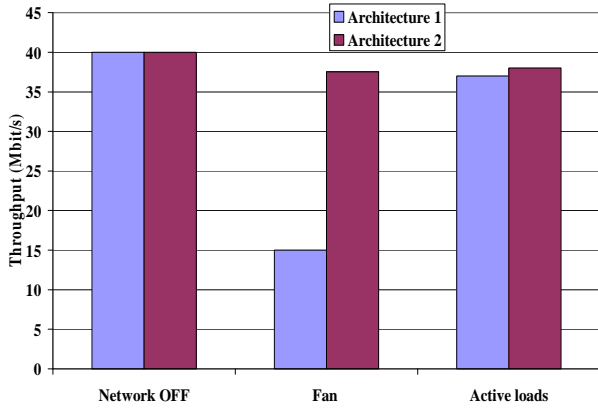


Figure 5. Throughput measurement

The minimum bit rate measured is about 15 Mbit/s. As specified in the communication buses like ARINC 429 [20], MIL-STD-1553 [21] and ARINC 825 [22], the required throughput for the FCS is about 1 Mbit/s. Thus, the results presented in Fig. 5 confirm the feasibility of the PLC technology in such application and thus it is possible to use PLC technology to convey such buses for FCS.

IV. INSERTION GAIN AND CHANNEL IMPULSE RESPONSE

In Section III, throughput is measured for the architectures 1 and 2. Even if this throughput is sufficient for FCS, the Homeplug Av standard is not adapted for the aircraft communication. In fact, the OFDM symbol duration is equal to 46.52 μ s, which is not in accordance with the real time constraints. Thus, we measured the channel transfer function to define new physical layer parameters adapted to this channel for a safety-critical aeronautical system.

A. Tested configurations

In Table I, the tested configurations are presented. “OFF” means that the power supply and the loads are connected to the network and they are turned off. “ON” means that the power supply and the loads are turned on. Transfer functions are measured between the two couplers. “P-to-p” means point-to-point and “P-to-m” means point-to-multipoint.

B. Channel measurement results

In this paragraph, we only show the transfer function with the network “ON” because there are no major differences between the transfer function with the network “OFF”. In addition, we do not represent the transfer function on the -270 V with the architecture 2 because, due to the symmetry of the network, transfer functions are similar on both polarities.

Fig. 6 represents the insertion gain (IG) for the point-to-point topology, namely, the architectures 1 and 2. For the architecture 1, which corresponds to the configurations C2 and C4, the IG decreases over the entire bandwidth with several resonances. For the architecture 2, which corresponds to the configuration C8, the IG first decreases linearly (in dB) with the frequency up to 40 MHz, and varies from -5 to -25 dB. Then, the IG remains nearly constant between 40 MHz and 80 MHz and, beyond 80 MHz, decreases very rapidly. Fig. 7 shows the cumulative distribution function (CDF) of the IG for the architectures 1 and 2. For the configuration C2 the insertion gain is higher than -23 dB over 50 % of the bandwidth and higher than -32 dB over 90 % of the entire bandwidth. For the configuration C4 the insertion gain is higher than -28 dB over 50 % of the bandwidth and higher than -35 dB over 90 % of the entire bandwidth

TABLE I. TESTED CONFIGURATIONS

	Configuration	Topology	Coupler	Polarity	Power	Loads
Architecture 1	C1	P-to-p	Capacitive	\pm	OFF	Active loads
	C2				ON	
	C3				OFF	
	C4				ON	
Architecture 2	C5		Inductive	-	OFF	Fan
	C6			+	OFF	
	C7			-	ON	
	C8			ON		
Architecture 3	C9	P-to-m		+	OFF	Active loads
	C10				OFF	Fan
	C11				ON	Active loads
	C12				ON	Fan

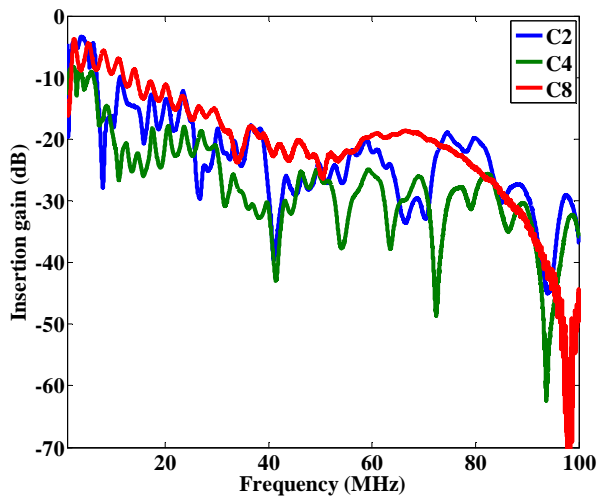


Figure 6. Insertion gain for the architectures 1 and 2

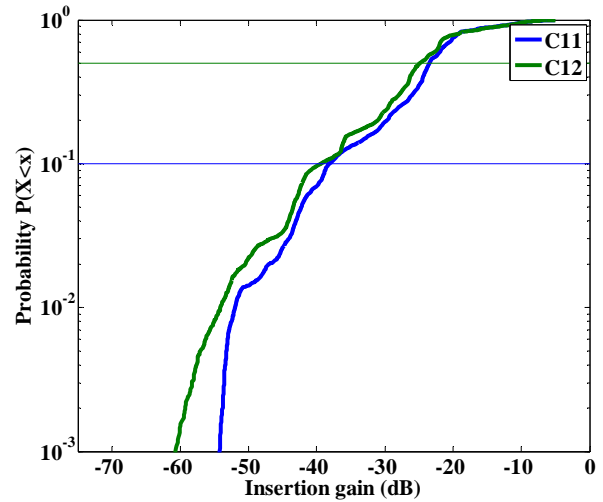


Figure 9. CDF the architecture 3

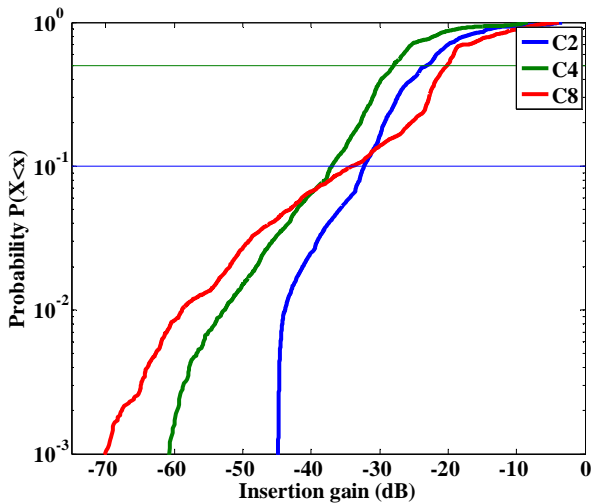


Figure 7. CDF the architectures 1 and 2

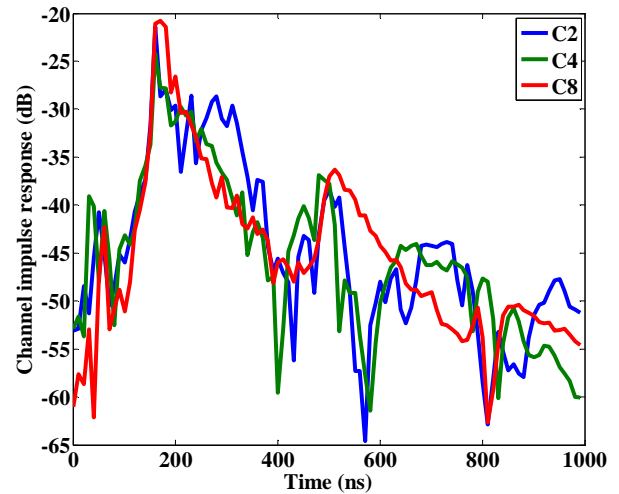


Figure 10. Channel impulse for architecture 1 and architecture 2 in the [1;100] MHz bandwidth

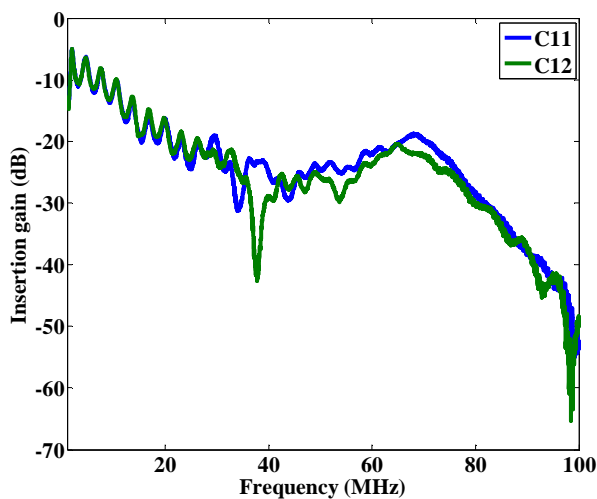


Figure 8. Insertion gain for the architecture 3

Fig. 8 represents the IG for the point-to-multipoint topology, namely, the architecture 3. The IG is quite similar for the two configurations. There is a resonance at about 39 MHz for configuration C12. The IG of the architecture 3 is few dB lower than the IG of the architecture 2. Finally, Fig. 9 shows the CDF for the architecture 3. For the configuration C2 the insertion gain is higher than -25 dB over 50 % of the bandwidth and higher than -39 dB over 90 % of the entire bandwidth.

The channel may be studied also in the time domain in order to get the impulse response. The channel impulse response has been obtained from the measurements of the complex transfer function by applying a 20000 points inverse Fourier transform (IFFT) in the [1;100] MHz bandwidth. The results of the channel responses for the architectures 1 and 2 are shown in Fig. 10.

Finally, the coherence bandwidth is calculated from the transfer function and the delay spread is calculated from the channel impulse response. The coherence bandwidth and the delay spread allow to define the subcarrier spacing and the cyclic prefix duration, respectively.

V. COHERENCE BANDWIDTH AND DELAY SPREAD

The coherence bandwidth is deduced from the absolute value of the autocorrelation of the complex transfer function [23]. The values of both coherence bandwidth and delay spread are calculated for 8 different frequency bandwidths for each configuration, from the [0;20] MHz bandwidth to the [0;100] MHz bandwidth with a step of 10 MHz. In the following, the coherence bandwidth is calculated for a correlation coefficient of 0.9. The delay spread is calculated from the channel impulse responses according to [24]. It appears that the values of the values of the coherence bandwidth and delay spread are quite independent of the frequency bandwidth analysis. Fig. 11 represents the coherence bandwidth versus the inverse of the delay spread for all the cases (bandwidths and configurations). Conventionally, the coherence bandwidth is proportional to the inverse of the delay spread. In our case, the linear regression leads to a correlation coefficient of 0.75. This result has been also noticed for indoor networks [25].

It appears that the architectures and the kind of coupler do not have a strong impact on the channel characteristics, the coherence bandwidth being of the order 700–1200 kHz, as the delay spread varies from 60 to 110 ns. These results are quite similar to those obtained for other embedded systems as shown in Table II. The delay spread measured for these channels is between 34 ns and 380 ns and the coherence bandwidth is between 0.4 MHz and 0.9 MHz.

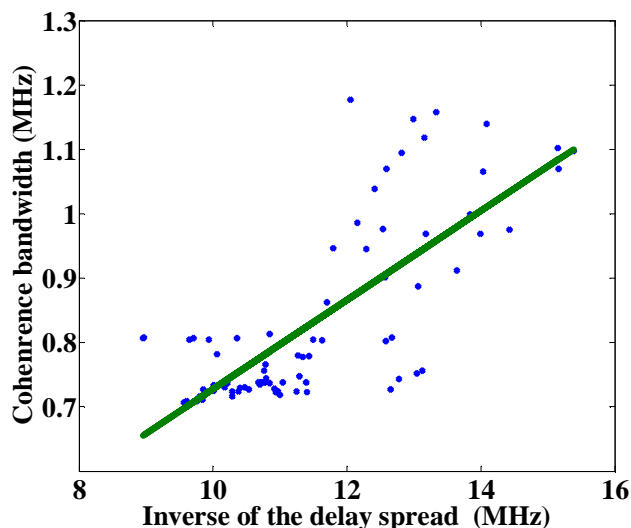


Figure 11. Coherence bandwidth versus of the inverse of delay spread

TABLE II. COHERENCE BANDWIDTH AND DELAY SPREAD FOR DIFFERENT VEHICLES

Vehicles References	Bandwidth (MHz)	Delay spread (ns)	Coherence bandwidth (MHz)
Car [15]	[1;50]	34-200	0.4-4.8
Aircraft [16]	[1;30]	100	0.6-0.9
Car[25]	[0.3;100]	130	0.48
Car [26]	[1;70]	380	0.4-0.7

VI. OPTIMIZATION OF OFDM PARAMETERS

Taking into account the obtained results, the next step is to adapt the OFDM symbol duration to the real time constraint. The real time constraint is defined by the duration between the moment when a bit enter in the transmitter and the moment when the same is available at the output of the receiver. We assume that all the information contained in an OFDM symbol must be completely received to be considered usable. As a result, the duration of the OFDM symbol is considered as an incompressible latency time. Thus, it is necessary to ensure that the OFDM symbol duration is lower than the real time constraints. It leads to an OFDM symbol duration between 17 μ s and 34 μ s, as explained in Section I. The OFDM symbol duration T_{OFDM} is given by the equation:

$$T_{OFDM} = \frac{1}{\text{sub carrier spacing}} + \text{cyclic prefix duration} \quad (1)$$

Thus, we need to adapt the sub-carrier spacing and the cyclic prefix duration (CP).

A. OFDM Sub-carrier Spacing

In order to meet the real time constraints, it is necessary to minimize the processing time for in the physical layer. Since fast Fourier transform (FFT) is a time consuming process proportional to the number of sub-carriers, one can try to decrease the number of carriers and choose, as in common practice, a sub-carrier spacing less than 10 % of the coherence bandwidth. Taking into account the values in Fig. 10, this leads to a 70 kHz sub-carrier spacing, which is about three times the value given in Homeplug Av specifications (24.414 kHz). To decrease the time processing, it is better to use a FFT size of power of 2. Finally, it is possible to switch off sub-carriers to transmit data on the proper frequency bandwidth. In our case, it leads to 428 or 1428 useful sub-carriers for a transmission bandwidth over 30 MHz or 100 MHz respectively.

B. Interference Characterization

Using the channel impulse response values, it is also possible to compute the inter symbol interference (ISI) and the inter carrier interference (ICI) according to the cyclic prefix CP length.

Then, it becomes possible to choose the optimal CP length because the increase of the CP length decreases the power spectral density of ISI and ICI but also reduces spectral efficiency and data rate. The power spectral density of ISI and ICI can be computed by the equation [27]:

$$I_{ISI+ICI}(n) = 2\sigma_x^2 \sum_{l=L_{cp}+1}^{L_c-1} \left| \sum_{u=l}^{L_c-1} h(u) \exp\left(-j \frac{2\pi}{N} un\right) \right|^2 \quad (2)$$

where σ_x^2 is the variance of modulated signal, h is the channel impulse response, L_c the channel length expressed in number of samples, L_{cp} being also expressed in terms of number of samples, N the number of sub-carriers, and n the frequency sample index.

Fig. 12 gives the normalized PSD interferences, expressed in dBm/Hz for configuration C11, which presents the highest delay spread, and calculated in the [1;30] MHz bandwidth. The PSD of the interferences has been plotted versus the sub-carrier index and for various lengths of the CP. As expected, the interference PSD decreases rapidly with the length of the cyclic prefix but, beyond 20 samples, it does not vary appreciably. Thus, it is not necessary to use a L_{cp} value higher than 20 samples.

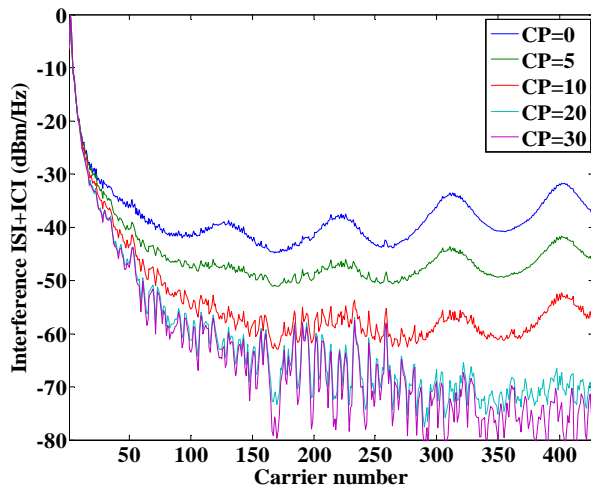


Figure 12. Interference in the [1-30] MHz bandwidth

C. Simulation Results

To show the influence of the CP length on the bit error rate (BER), an OFDM transmission chain has been simulated using Matlab. The simulated transmission chain is presented in Fig. 13. The first block of the transmitter is a random binary data generator. The generated data are mapped using binary phase shift keying (BPSK) modulation and an IFFT is then applied. The CP is then added to the OFDM symbol in the time domain. The channel includes both the complex channel impulse response and the additive white Gaussian noise (AWGN). At the receiver, the inverse process is realized and an equalization is used to compensate the distortion effect introduced by the channel. For these simulations, the channel estimation is assumed to be ideal and the zero forcing equalization is applied [28].

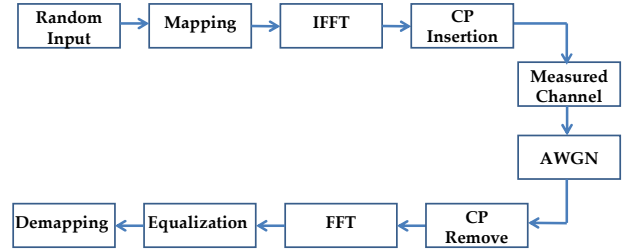


Figure 13. simulated OFDM transmission and reception chain

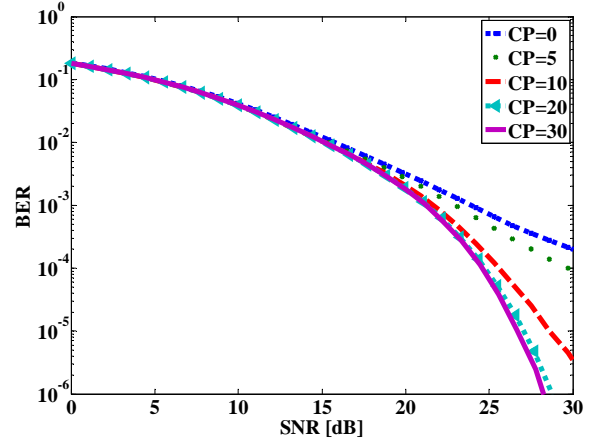


Figure 14. BER for different cyclic prefix length

The time and frequency synchronization are assumed to be perfect. Each useful sub-carrier transmits one bit corresponding to a BPSK symbol. In the following simulations, the configuration C11 is tested over the [0;36] MHz bandwidth and all the sub-carriers in the [30;36] MHz bandwidth are turned off. The SNR is defined as the ratio between the received power and the noise power. Fig. 14 shows the influence of the CP length (in number of samples) on the BER. In this configuration, the sub-carrier spacing is equal to 70 kHz. The degradation of the BER increases when the CP length decreases. One can observe that a CP length of 20 samples allows to absorb the interference due to the multipaths, as expressed in the Section VI.B. Taking into account the interferences and the BER calculations, we propose a CP duration of 20 samples, which correspond to 666 ns on the [1;30] MHz bandwidth. As a comparison, if the cyclic duration was chosen equal to 2 to 4 times the delay spread, as suggested in [29], we would obtain a CP duration between 220 and 440 ns, which is not sufficient in our case as observed in Fig. 14.

VII. SYNTHESIS AND CONCLUSION

In this paper, we have studied the feasibility of PLC transmissions for avionic safety critical systems. Throughput measurements with Homeplug Av modems have been done and show a sufficient throughput for the FCS. In addition, the channel measurements prove that it is possible to reduce the duration of an OFDM symbol, compared to the Homeplug Av standard, by both increasing the sub-carrier spacing and decreasing the cyclic prefix

duration. In fact, in the Homeplug Av standard, the sub-carrier spacing is 24.414 kHz, the minimum cyclic prefix duration is 5.56 μ s, and the OFDM symbol duration is 46.52 μ s. In this PLC application, we propose to increase the sub-carrier spacing up to 70 kHz and to decrease the CP duration to 666 ns. Consequently, the OFDM symbol duration is 14.94 μ s. These results will help us to define the physical layer parameters for a PLC avionics system in accordance with real-time constraints of a fast control loop. This study can be applied to other critical avionic systems running on a HVDC network like landing gear. It is also possible to use this study for a slow control loop on HVDC network like thrust reversal.

In the next steps, we will continue to define the OFDM parameters (constellation and frequency bandwidth) and the channel coding to ensure a sufficient quality of the service for the FCS. In addition of the real time constraint, the quality of service that is defined by the useful bitrate (10 Mbit/s), the bit error rate (10^{-12} as on the AFDX), and the respect of the DO-160 gauge in conducted emissions may be taken into account in the parameters of the physical layer.

ACKNOWLEDGMENT

This study is funded by Safran and followed by IETR of Rennes.

REFERENCES

- [1] T. Larhzaoui, F. Nouvel, J.Y. Baudais, V. Déguardin and P. Laly, "Analysis of PLC channels in aircraft environment and optimization of some OFDM parameters," International Conference on Systems and Networks Communications, pp. 65-69, October 2013.
- [2] A. Garg, R.I Linda and T. Chowdhury, "Application of fiber optics in aircraft control system & its development," *International Conference on Electronics and Communication Systems (ICECS)*, pp. 1-5, February 2014.
- [3] D. Dinh-Khanh, A. Mifdaoui and T. Gayraud, "Fly-By-Wireless for next generation aircraft: Challenges and potential solutions," *Wireless Days (WD)*, pp. 1-8, 21-23 November 2012.
- [4] HomePlug Av specification, Version 1.1, May 2007.
- [5] J. Granado, A. Torralba and J. Chavez, "Using broadband power line communications in non-conventional applications," *IEEE Transactions on consumer electronics*, vol. 57, no. 3, pp. 1092-1098, August 2011.
- [6] P. Tanguy and F. Nouvel, "In vehicle PLC simulator based on channel measurements," *Intelligent Transport Systems Telecommunications*, pp. 9-11, November 2010.
- [7] G. Sung, C. Huang and C. Wang, "A PLC transceiver design of in-vehicle power line in FlexRay-based automotive communication systems," *IEEE International Conference on Consumer Electronics*, vol. 13, no. 16, pp. 309-310, January 2012.
- [8] M. Mohammadi, L. Lampe, M. Lok, S. Mirabbasi, M. Mirvakili, R. Rosales and P. van Veen, "Measurement study and transmission for in-vehicle power line communication," *IEEE International Symposium on Power Line Communications and Its Applications*, pp. 73-78, March 2009.
- [9] S. Barmada, L. Bellanti, M. Raugi, and M. Tucci, "Analysis of power-line communication channels in ships," *IEEE Transactions on Vehicular Technology*, vol. 59, no. 7, pp. 3161-3170, September 2010.
- [10] M. Antoniali, A. Tonello, M. Lenardon and A. Qualizza, "Measurements and analysis of PLC channels in a cruise ship," *IEEE International Symposium on Power Line Communications and Its Applications*, vol. 3, no. 6, pp.102-107, April 2011.
- [11] A. Akinnikawe and K. Butler-Purry, "Investigation of broadband over power line channel capacity of shipboard power system cables for ship communication networks," *IEEE Power & Energy Society General Meeting*, pp.1-9, July 2009.
- [12] S. Barmada, A. Gaggelli, A. Musolino, R. Rizzo, M. Raugi and M. Tucci, "Design of a PLC system onboard trains: Selection and analysis of the PLC channel," *IEEE International Symposium on Power Line Communications and Its Applications*, vol. 2, no. 4, pp. 13-17, April 2008.
- [13] K. Liu D. Jiang, "PLC used in the train control simulation system," *IEEE International Conference on Computer Science and Automation Engineering*, vol. 2, no. 25-27, pp. 308-311, May 2012.
- [14] S. Bertuol, I. Junqua, V. Degardin, P. Degauque, M. Lienard, M. Dunand and J. Genoulaz, "Numerical assessment of propagation channel characteristics for future application of power line communication in aircraft," *EMC Europe*, pp. 506-511, September 2011.
- [15] V. Degardin, I. Junqua, M. Lienard, P. Degauque and S. Bertuol, "Theoretical Approach to the Feasibility of Power-Line Communication in Aircrafts," *IEEE Transactions on Vehicular Technology*, vol. 62, no. 3, pp. 1362-1366, March 2013.
- [16] K. Kilani, V. Degardin, P. Laly, M. Lienard and P. Degauque, "Impulsive noise generated by a pulse width modulation inverter: modeling and impact on powerline communication," *IEEE International Symposium on Power Line Communications and Its Applications*, pp. 75-79, March 2013.
- [17] DO-160, "Environmental conditions and test procedures for airborne equipment," RTCA Inc., 2007.
- [18] K. Fazel and S. Kaiser, *Multi-Carrier and Spread Spectrum Systems: From OFDM and MC-CDMA to LTE and WiMAX*, John Wiley & Sons Ltd, 2008.
- [19] ARINC 664, "Aircraft data network part 7 avionics full duplex switched ethernet (AFDX) network," Arinc specification 664 P, Jun 2005.
- [20] Arinc 429, "Specification Tutorial", AIM GmbH, July 2001.
- [21] "An Interpretation of MIL-STD-1553B," SBS Technologies Inc.
- [22] R. Kneuppel, "Standardisation of CAN network for airborne use through ARINC 825," *International CAN Conference*, pp.1-8, March 2012.
- [23] T.S. Rappaport, *Wireless communication principle and practice*, Prentice Hall, 1996.
- [24] M. Tlich, G. Avril and A. Zeddou, "Coherence bandwidth and its relationship with the rms delay spread for PLC channels using measurements up to 100 MHz," *Home networking, International Federation for Information Processing*, vol. 256, pp. 129-142, January 2008.
- [25] A.B. Vallejo-Mora, J.J. Sanchez-Martinez, F.J. Canete, J.A. Cortés and L. Diez, "Characterization and evaluation of in-vehicle power line channels," *IEEE Global Telecommunications Conference*, pp. 1-5, December 2010.
- [26] M. Lienard, M. Olivas Carrion, V. Degardin, and P. Degauque, "Modeling and analysis of in-vehicle power line communication Channels," *IEEE Transaction on Vehicular Technology*, vol. 57, no. 2, pp. 670-679, March 2008.
- [27] W. Henkel, G. Taubock, P. Odling, P.O. Borjesson and N. Petersson, "The cyclic prefix of OFDM/DMT. An analysis," *International Zurich Seminar on Broadband Communications, Access, Transmission, Networking*, pp. 22-1-22-3, September 2002.
- [28] G. Proakis, *Digital communication*, McGraw Hill series in electrical and computer engineering, 1996.
- [29] R. Van Nee and R. Prasad, *OFDM for wireless multimedia communications*, Artech House, 2000.